Electronic Supplementary Material (ESI) for Materials Horizons.
This journal is © The Royal Society of Chemistry 2021

Electronic Supplementary Information

Unveiling the Crucial Contributions of Electrostatic and Dispersion Interactions to the Ultralong Room-Temperature Phosphorescence of H-bond Crosslinked Poly(vinyl alcohol) Films

Deliang Wang[a,b], Hongzhuo Wu[a,b], Junyi Gong[d], Yu Xiong*[a, c], Qian Wu[a,b], Zheng Zhao[d], Lei Wang[a], Dong Wang*[a], Ben Zhong Tang*[c,d]

[a] *Center for AIE Research, Shenzhen Key Laboratory of Polymer Science and Technology, Guangdong Research Center for Interfacial Engineering of Functional Materials, College of Materials Science and Engineering, Shenzhen University, Shenzhen 518061, China*

[b] *Key Laboratory of Optoelectronic Devices and Systems of Ministry of Education and Guangdong Province, College of Physics and Optoelectronic Engineering, Shenzhen University, Shenzhen 518061, China. E-mail: xiongyu@szu.edu.cn; E-mail: wangd@szu.edu.cn*

[c] *HKUST Shenzhen Research Institute, Shenzhen 518057, China*

[d] *Shenzhen Institute of Molecular Aggregate Science and Engineering, School of Science and Engineering, The Chinese University of Hong Kong, Shenzhen 518172, China.*

E-mail: tangbenz@cuhk.edu.cn

Table of Contents

1. General methods

1.1 Instruments: The UV-vis absorption spectra were recorded on a UV-2600 spectrophotometer. The photoluminescence spectra were recorded on a PerkinElmer LS 55 fluorescence spectrometer. Absolute quantum yields, and the lifetimes of fluorescence and phosphorescence spectra were measured on the Edinburgh FLS1000 fluorescence spectrophotometer equipped with a continuous xenon lamp (Xe1), a microsecond pulsed xenon flashlamp (uF920), and a nanosecond flashlamp lamp (nF920), respectively. The photos and videos were recorded by a mobile phone iPhone 8. High-performance liquid chromatography (HPLC) was performed on the Agilent 1260 infinity II HPLC system. The running buffer: 0.05%TFA-H2O/0.04%TFA-ACN (TPB-3COOH and TPB-3OH); 0.03%TFA-95%H2O-5%ACN/0.03%TFA-95%ACN-5%H2O (TPB-3NH2).

1.2 Theoretical calculation methods: Theoretical calculations were performed at B3LYP/6-31G (d, p) level using the Gaussian 09 program packages (Revision D 01).[1] The energy decomposition analysis was calculated by symmetry-adapted perturbation theory (SAPT) under SAPT0/jun-cc-pVDZ level of corresponding compounds with segment from polyvinyl alcohol in Psi4 software package.[2-4] The total intermolecular interaction energy can be decomposed into electrostatic, induction, dispersion and repulsion energies. The electrostatic potential (ESP) pictures were obtained from Gauss View 5 with an electron density isosurface value of 0.001. Polarizability was calculated at B3LYP/def2-SVPD level.

1.3 Single-crystal structures: the crystallographic data of guest molecules TPB-3COOH (Deposition Number: 1400565) and TPB-3OH (Deposition Number: 173734) and TPB-3NH2 (Deposition Number: 940123) have been reported in previous literatures.[5-7]

1.4 The method of obtaining the absolute photoluminescence quantum yields: the absolute photoluminescence quantum yields (PLQY) of all the doped PVA films were measured on the Edinburgh FLS1000 fluorescence spectrophotometer with an integrating sphere under ambient conditions. The phosphorescence quantum yields all the doped PVA films were obtained following the equation

$$\phi_{phos} = \frac{B}{A} \times \phi_{PL}$$

where A and B represent the integral areas of total photoluminescence and phosphorescence spectra, respectively. The phosphorescence was separated from total PL spectrum on the basis of phosphorescence spectrum for phosphorescence quantum yields. This method has been reported in previous literature.[8]

2. Supporting Figures and Tables

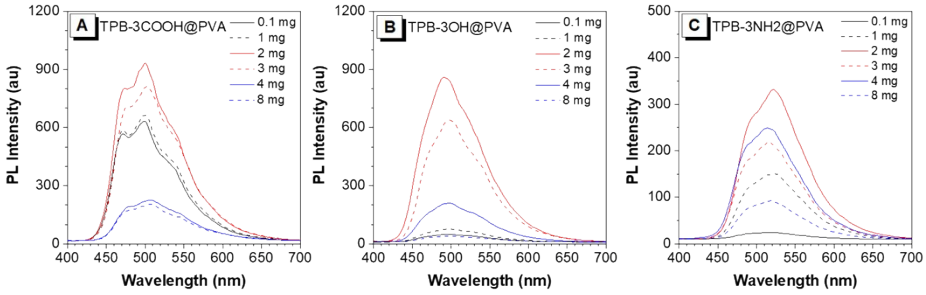

Figure S1. (A-C) Concentration dependence of phosphorescence spectra of doped PVA films at room

temperature.

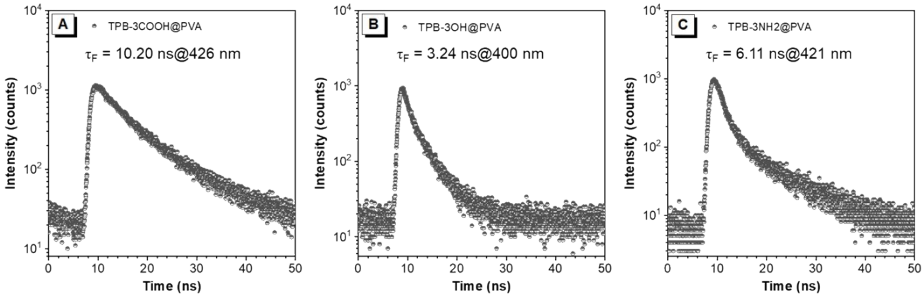

Figure S2. (A-C) Time-resolved fluorescent decay curves of doped PVA films at room temperature (excitation wavelength: 320 nm).

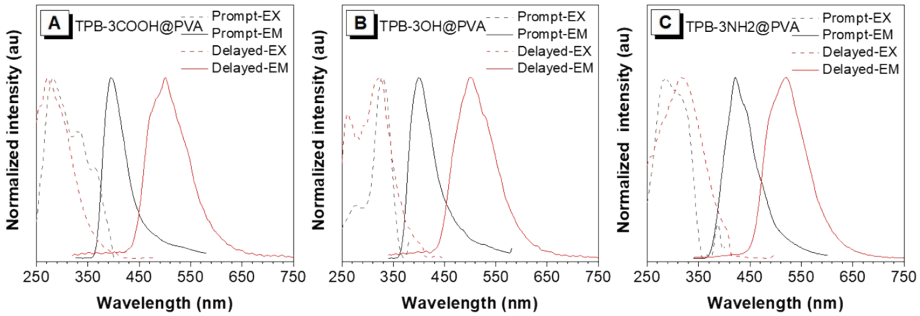

Figure S3. (A-C) Normalized excitation and emission spectra of doped PVA films at room temperature.

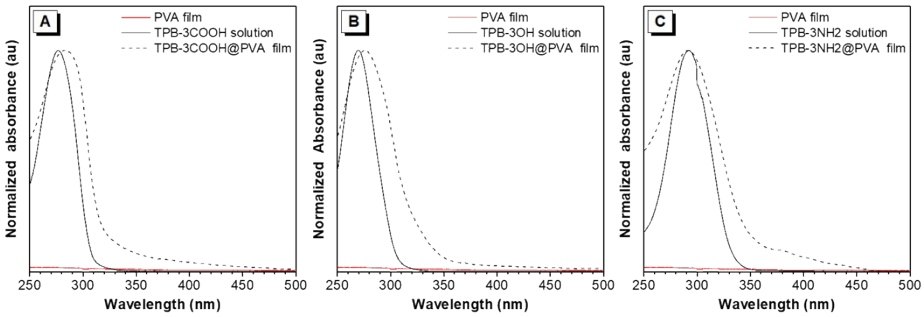

Figure S4. (A-C) Superposed absorption spectra of PVA film, organic guest molecules in dilute solution and doped PVA films.

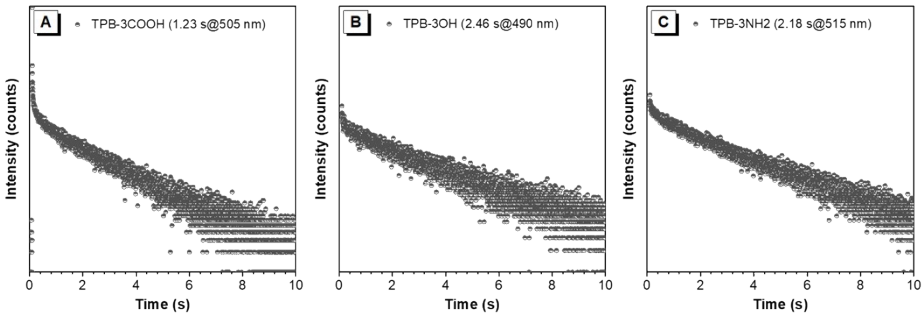

Figure S5. (A-C) Time-resolved phosphorescent decay curves of guest molecules in dilute THF solutions at 77 K.

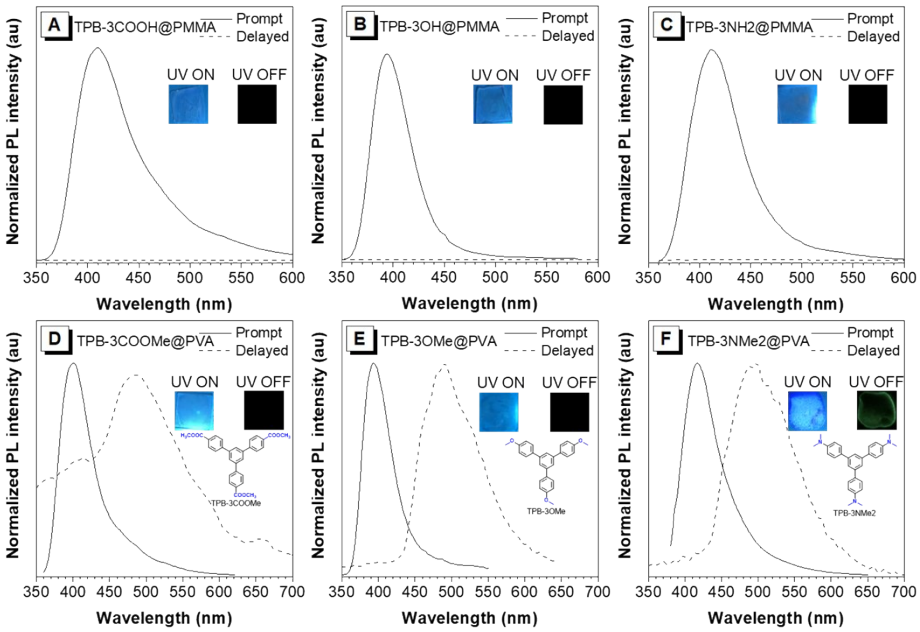

Figure S6. (A-C) Prompt and delayed PL spectra of doped PMMA films; (D-F) prompt and delayed PL spectra of doped PVA films based on the guest molecules TPB-3COOMe, TPB-3OMe and TPB-3NMe2, respectively (inset image: luminescence photographs of doped films under UV irradiation and after removal of UV irradiation).

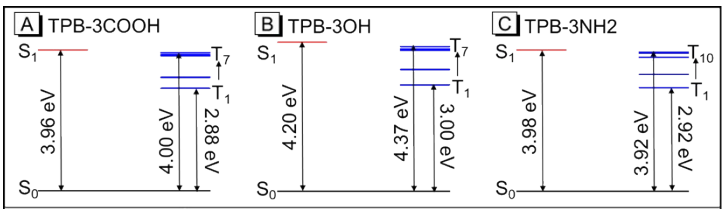

	SOC (cm^{-1})		
	TPB-3COOH	TPB-3OH	TPB-3NH2
S0-T1	0.32	0.32	0.37
S1-T1	0.61	0.26	0.33
S1-T2	0.08	0.04	0.04
S1-T3	0.26	0.04	0.04
S1-T4	0.14	0.24	0.34
S1-T5	0.24	0.07	0.28
S1-T6	0.11	0.06	0.17
S1-T7	0.03	0.00	0.06
S1-T8	/	/	0.16
S1-T9	/	/	0.25
S1-T10	/	/	0.31

Figure S7. (A-C) The energy level diagrams, spin-orbit coupling (SOC) constants between the S_0/S_1 and involved T_n states of guest molecules TPB-3COOH, TPB-3OH, and TPB-3NH2 calculated in the gas phase.

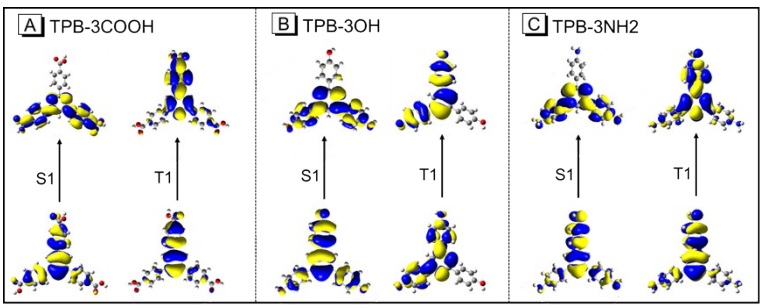

Figure S8. (A-C) The natural transition orbital (NTO) distributions of guest molecules TPB-3COOH, TPB-3OH, and TPB-3NH2 calculated in the gas phase.

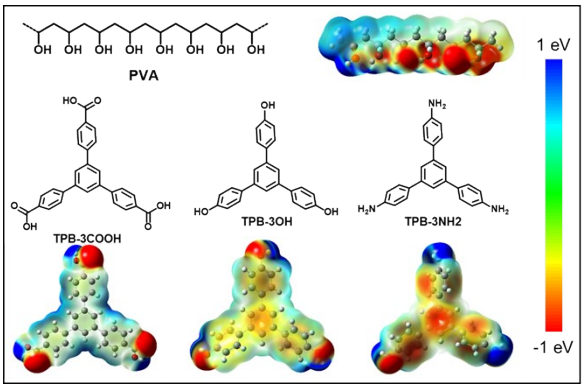

Figure S9. Calculated electrostatic potential (ESP) distributions of guest molecules.

Table S1. Photophysical properties of doped PVA films at room temperature.

Doped films	λ_F [nm]	λ_P [nm]	τ_F [ns]	τ_P [s]	Φ_F [%]	Φ_P [%]	k_F [s^{-1}]	k_P [s^{-1}]	k_{NR} [s^{-1}]
TPB-3COOH@PVA	394	500	10.20	1.03	11.36	2.98	1.11×10^{7}	2.89×10^{-2}	0.94
TPB-3OH@PVA	400	500	3.24	1.31	11.67	2.25	3.60×10^{7}	1.73×10^{-2}	0.75
TPB-3NH2@PVA	421	519	6.11	1.74	7.56	1.41	1.24×10^{7}	8.10×10^{-3}	0.57

λ_F: fluorescence emission; λ_P: phosphorescence emission; τ_F: fluorescence lifetime; τ_P: phosphorescence lifetime; Φ_F: fluorescence quantum yield; Φ_P: phosphorescence quantum yield; k_F: radiative decay rate of fluorescence; k_P: radiative decay rate of phosphorescence; k_{NR}: nonradiative decay rate of phosphorescence; $k_F = \Phi_F/\tau_F$; $k_P = \Phi_P/\tau_P$; $k_{NR} = (1-\Phi_P)/\tau_P$.

Table S2. Calculated complexation energies and corresponding energy decomposing analysis data of different complexation modes between the guest molecules and PVA matrix.

Complexation	Interaction energy (kcal mol^{-1})	TPB-3COOH@PVA	TPB-3OH@PVA	TPB-3NH2@PVA
Mode A	Electrostatic	-29.99	-27.95	-8.78
	Induction	-12.99	-11.52	-1.83
	Dispersion	-9.09	-9.13	-4.29
	Exchange	29.06	30.65	7.60
	$E_{complex}$	-23.01	-17.95	-7.30
Mode B	Electrostatic	-18.25	-18.93	-23.44
	Induction	-7.70	-8.80	-10.12
	Dispersion	-26.00	-25.28	-26.53
	Exchange	35.67	35.93	39.80
	$E_{complex}$	-16.28	-17.08	-20.29

Table S3. Calculated polarizability of guest molecules.

Guest molecule	Polarizability (10^{-40} *C. m². V⁻¹*)
TPB-3COOH	62.96
TPB-3OH	53.64
TPB-3NH2	58.21

Purity characterizations of compounds TPB-3COOH, TPB-3OH, and TPB-3NH2.

Compound TPB-3COOH: ^{1}H NMR (500 MHz, d_6-DMSO) δ (ppm): 8.04–8.09 (m, 15H). Elemental analysis calcd for $C_{27}H_{18}O_6$: C, 73.97; H, 4.14. Found: C, 73.62; H, 4.12.

Compound TPB-3OH: ^{1}H NMR (500 MHz, d_6-DMSO) δ (ppm): 9.61 (s, 3H), 7.62–7.64 (m, 9H), 6.87–6.89 (d, 6H). Elemental analysis calcd for $C_{24}H_{18}O_3$: C, 81.34; H, 5.12. Found: C, 81.22; H, 5.04.

Compound TPB-3NH2: ^{1}H NMR (500 MHz, d_6-DMSO) δ (ppm): 7.48–7.49 (m, 9H), 6.66–6.68 (d, 6H), 5.20 (s, 6H). Elemental analysis calcd for $C_{24}H_{21}N_3$: C, 82.02; H, 6.02; N, 11.96. Found: C, 81.83; H, 5.82; N, 11.84.

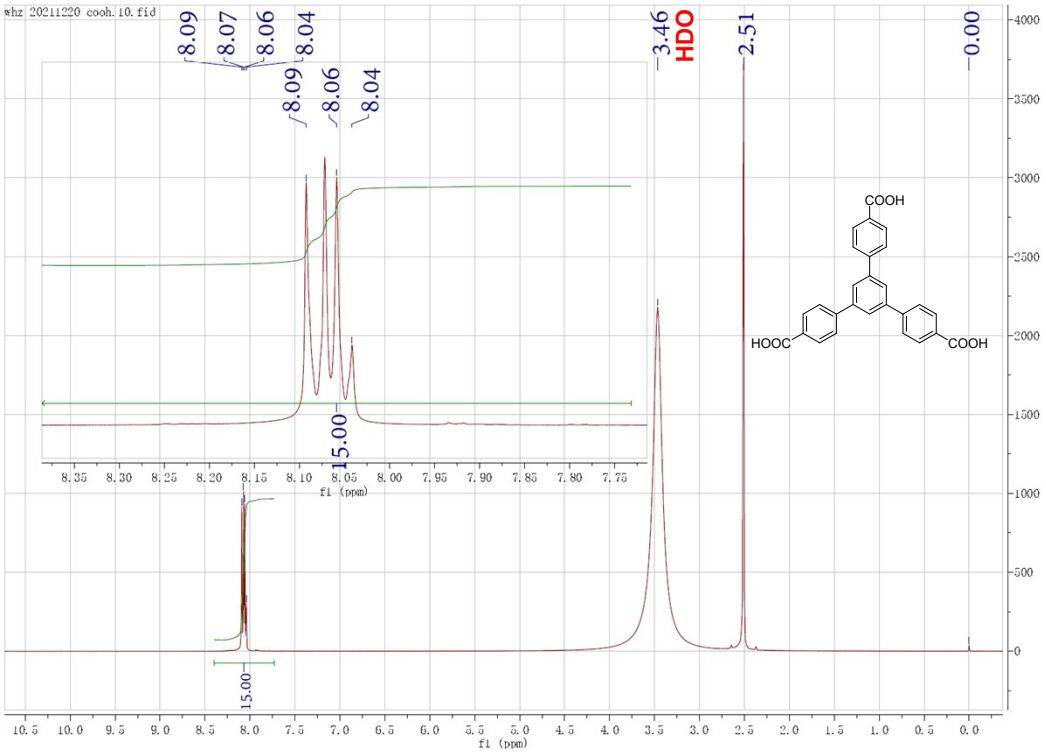

Figure S10. ^{1}H NMR spectrum of compound TPB-3COOH in d_6-DMSO.

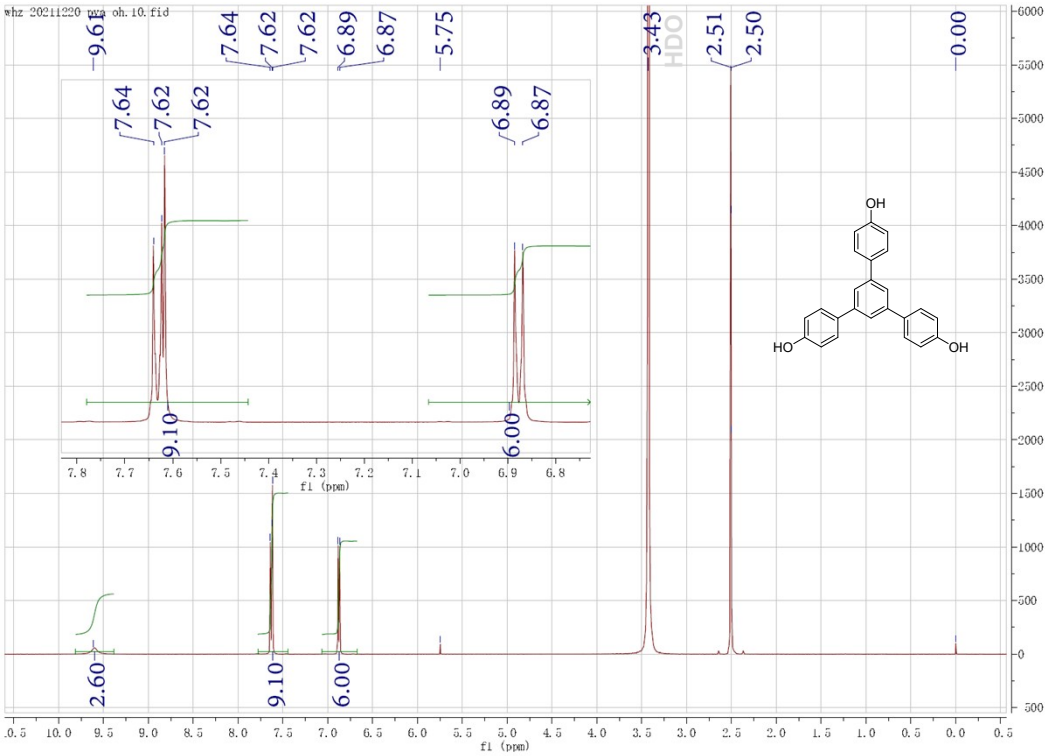

Figure S11. ^{1}H NMR spectrum of compound TPB-3OH in d_6-DMSO.

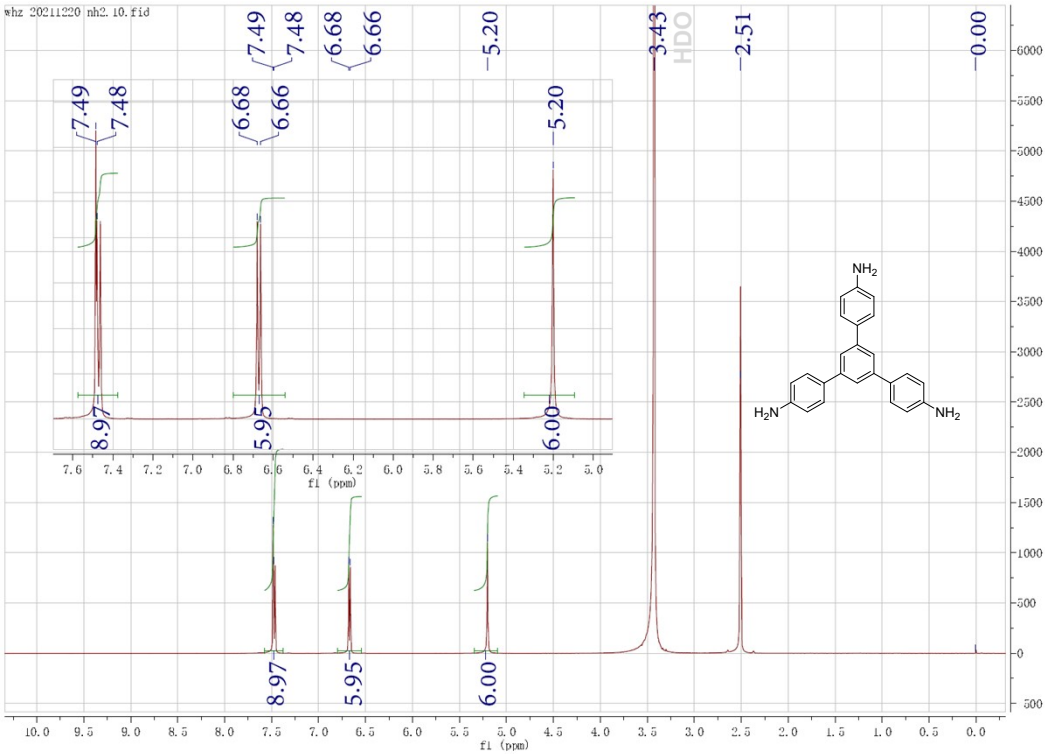

Figure S12. ^{1}H NMR spectrum of compound TPB-3NH2 in d_6-DMSO.

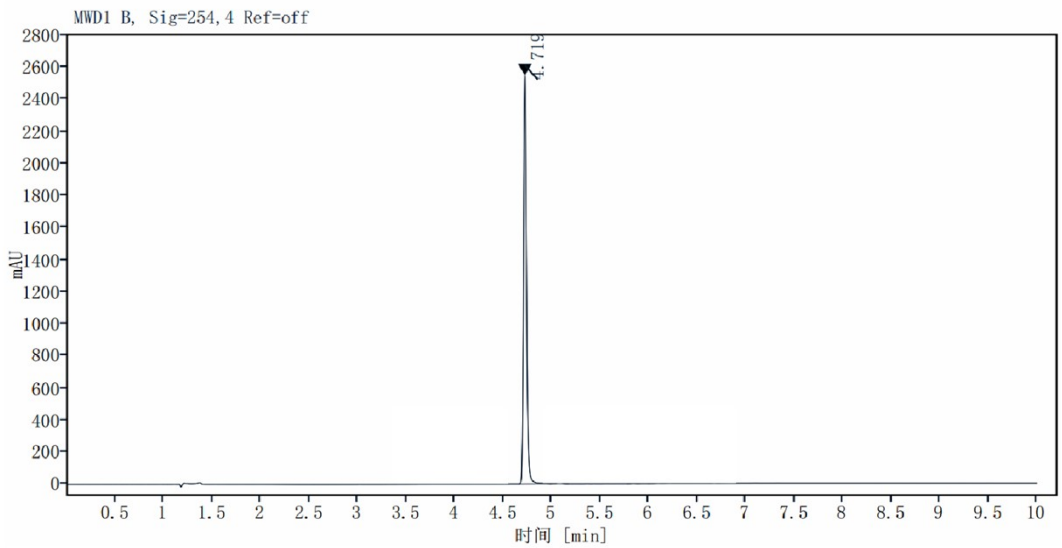

Figure S13. High-performance liquid chromatography diagram of compound TPB-3COOH.

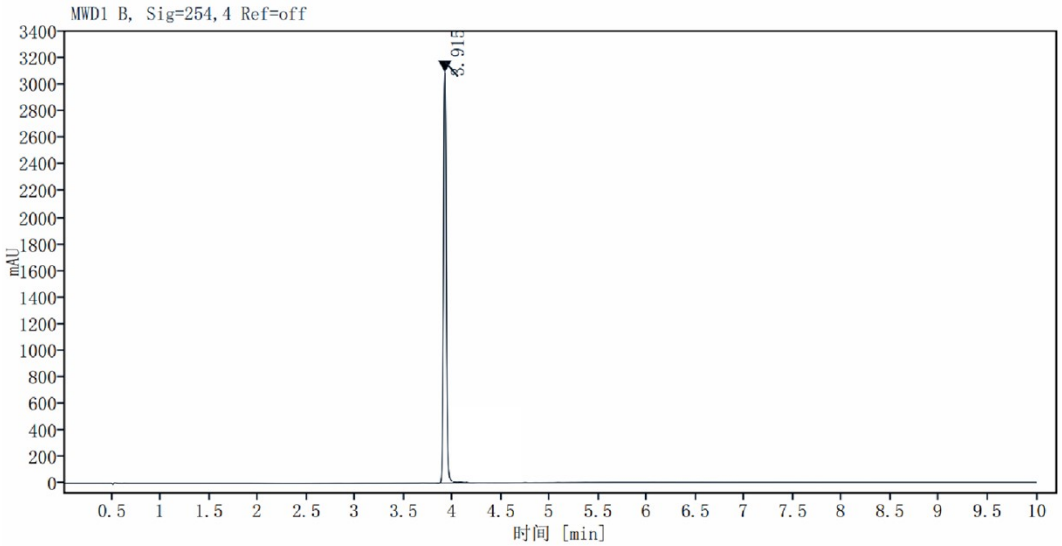

Figure S14. High-performance liquid chromatography diagram of compound TPB-3OH.

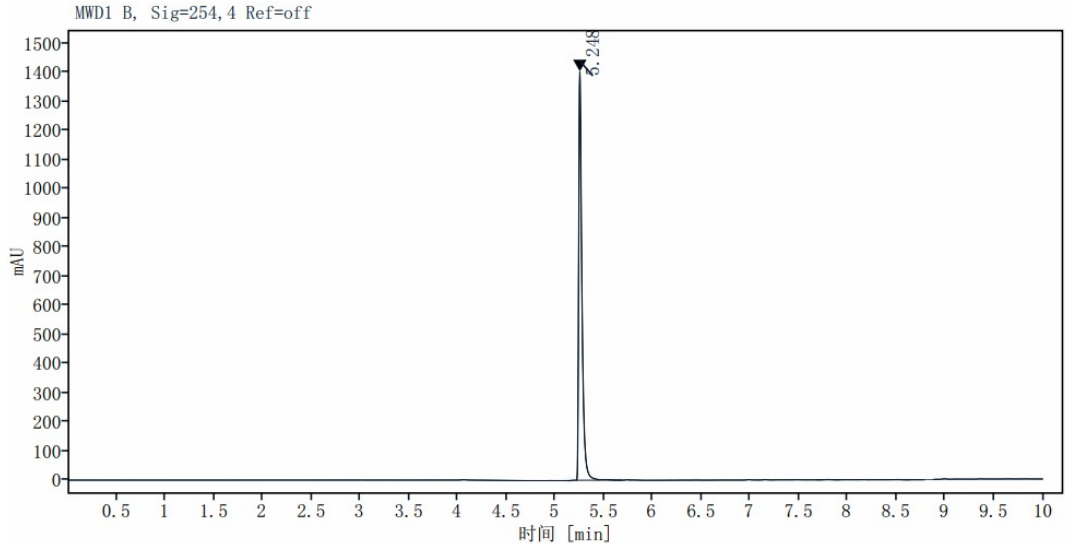

Figure S15. High-performance liquid chromatography diagram of compound TPB-3NH2.

3. References

1. M. J. Frisch, G. W. Trucks, H. B. Schlegel, G. E. Scuseria, M. A.Robb, J. R. Cheeseman, G. Scalmani, V. Barone, B. Mennucci, G. A. Petersson, H. Nakatsuji, M.Caricato, X. Li, H. P. Hratchian, A. F. Izmaylov, J. Bloino, G. Zheng, J. L. Sonnenberg, M. Hada, M. Ehara, K. Toyota, R. Fukuda, J. Hasegawa, M. Ishida, T. Nakajima, Y. Honda, O. Kitao, H.Nakai, T. Vreven, J. A. Montgomery, Jr., J. E. Peralta, F. Ogliaro, M. Bearpark, J. J. Heyd, E.Brothers, K. N. Kudin, V. N. Staroverov, T. Keith, R. Kobayashi, J. Normand, K. Raghavachari, A. Rendell, J. C. Burant, S. S. Iyengar, J. Tomasi, M. Cossi, N. Rega, J. M. Millam, M. Klene, J.E. Knox, J. B. Cross, V. Bakken, C. Adamo, J. Jaramillo, R. Gomperts, R. E. Stratmann, O. Yazyev, A. J. Austin, R. Cammi, C. Pomelli, J. W. Ochterski, R. L. Martin, K. Morokuma, V. G. Zakrzewski, G. A. Voth, P. Salvador, J. J. Dannenberg, S. Dapprich, A. D. Daniels, O. Farkas, J. B. Foresman, J. V. Ortiz, J. Cioslowski, and D. J. Fox, Gaussian, Inc., Wallingford CT, **2013**.

2. R. M. Parrish, L. A. Burns, D. G. A. Smith, A. C. Simmonett, A. E. DePrince III, E. G. Hohenstein, U. Bozkaya, A. Y. Sokolov, R. Di Remigio, R. M. Richard, J. F. Gonthier, A. M. James, H. R. McAlexander, A. Kumar, M. Saitow, X. Wang, B. P. Pritchard, P. Verma, H. F. Schaefer III, K. Patkowski, R. A. King, E. F. Valeev, F. A. Evangelista, J. M. Turney, T. D. Crawford, and C. D. Sherrill, *J. Chem. Theory Comput.* 2017, **13**, 3185-3197.

3. D. G. A. Smith, L. A. Burns, A. C. Simmonett, R. M. Parrish, M. C. Schieber, R. Galvelis, P. Kraus, H. Kruse, R. D. Remigio, A. Alenaizan, A. M. James, S. Lehtola, J.P. Misiewicz, M. Scheurer, R. A. Shaw, J. B. Schriber, Y. Xie, Z. L. Glick, D. A. Sirianni, J. S. O'Brien, J. M. Waldrop, A. Kumar, E. G. Hohenstein, B. P. Pritchard, B. R. Brooks, H. F. Schaefer III, A. Y. Sokolov, K. Patkowski, A. E. DePrince III, U. Bozkaya, R. A. King, F. A. Evangelista, J. M. Turney, T. D. Crawford, and C. D. Sherrill2, *J. Chem. Phys.* 2020, **152**, 184108-184113.

4. B. Jeziorski, R. Moszynski, and K. Szalewicz, *Chem. Rev.* 1994*,* **94***,* 1887-1930.

5. C. A. Zentner, H. W. H. Lai, J. T. Greenfield, R. A. Wiscons, M. Zeller, C. F. Campana, O. Talu, S. A. FitzGeralde, J. L. C. Rowsell, *Chem. Commun.* 2015*,* **51***,* 11642-11645.

6. P. K. Thallapally, A. K. Katz, H. L. Carrellb, G. R. Desiraju, *Chem. Commun.* 2002*,* **4***,* 344-345.

7. P. Vishnoi, M. G. Walawalkar, R. Murugavel, *Cryst. Growth Des.* 2014*,* **14***,* 5668–5673.

8. Z. Yin, M. Gu, H. Ma, X. Jiang, J. Zhi, Y. Wang, H. Yang, W. Zhu, Z. An, *Angew. Chem. Int. Ed*. 2021, **60**, 20058.